STABILITY ANALYSIS OF GYROSCOPIC POWER GENERATOR

Satoru Yoshikawa[1], Tomohiro Ishii[1], Jun Iwasaki[1], Hiroshi Hosaka[1]
[1]Dept. of Human and Engineered Environmental Studies , Graduate School of Frontier Sciences, the University of Tokyo, Chiba, Japan

Abstract: Dynamics of a rotor used for the gyroscopic power generator is studied which generates high speed rotation of magnets through precession using vibrations of human body in daily life. First the approximate solution for the steady state rotation is obtained in a simple formulus. Next the transient response of the rotator is numerically analyzed by solving Eulerian equations. As a result, it was found that the stable rotation appears only for some amplitude and frequency of input vibration, and under some initial conditions which exist discontinuously state solution.

Key words: precession movement, electromagnetic power generation, gyroscopic power generator

1. INTRODUCTION

In order to solve the energy supply problem for ubiquitous equipments, many power generation systems utilizing energy in nature or from some artifacts have been presented. [1] Especially a power supply for small wireless sensors attached to moving bodies such as human is in requisition. A solution is a generator using vibration of moving bodies. Low level vibrations occur in many environments so it can generate electric power at various locations. Generally potential power of it is proportional to oscillatory mass and the square of oscillating velocity. Thus with a simple oscillator, it is difficult to make a small and high power generator that operates under low level vibration. To solve this problem, a gyroscopic power generator has been presented which generates high speed rotation of the rotor utilizing precession and friction[2] . Although this generator can produce around 1 W from input frequency of 2 Hz, it has a defect that the rotation is not stable and easily stalls depending on vibrational conditions. Thus it is necessary to clarify the condition for stable rotation.

In this paper, first, the structure and power generation principle of the gyroscopic generator is explained. Next, a dynamic model of the device is presented and an approximate solution for steady state rotation is obtained. Then, the transient response of the generator is numerically calculated. With these analyses, relationships between stable rotation and rotor parameters, amplitude and frequency of input vibration, initial condition of rotation are clarified.

2. GENERATOR CONFIGURATION

In this section principle of the gyroscopic power generator is presented. Figure 1 shows the composition of the generator. There is a rotor with magnets that rotates y axially at ω_y, and z axially at ω_z. The shaft of the rotor is supported by tracks convolved with coil. The gap of the tracks is slightly larger than the diameter of the shaft. When the track is rotated x axially at ω_x, the torque in the direction of ω_x is produced for the rotor, and the rotor starts precession movement ω_y by the law of angular momentum. Then, the shaft is applied the frictional force from the track. Figure 2 shows the generator seen x axially.

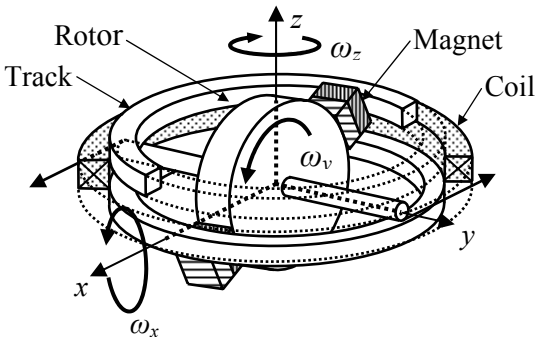

Fig.1 : Structure of gyroscopic generator.

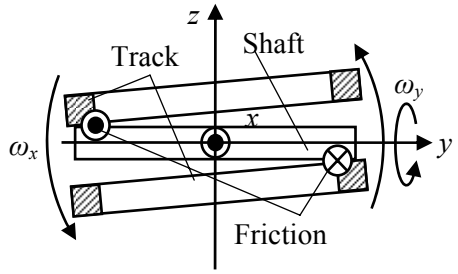

Fig. 2 : Principle for increase of spinning velocity.

The shafts contact only with one of track sides because there is a space between tracks. The frictional force generates the torque in the direction where rotation ω_y of the rotor is increased. As a result, the rotor spinning speed increases as the track is rotated and vibrated.

This principle of operation is used in the toy "Dynabee" [3][4]. Figure 3 shows the generator seen y axially. Since the rotor shaft changes direction by precession, the coil and the rotor are arranged perpendicularly. By rotating magnets, the magnetic field in the coil surface is changed and the alternative voltage is generated in the coil.

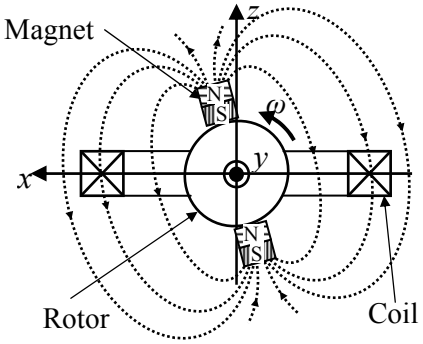

Fig 3 : Magnetic-field distribution.

3. THEORY AND STEADY STATE SOLUTION

To analyze the intricate rotation, we define some coordinate systems, as shown in Figure 4. A right-handed orthogonal coordinate system ***E*** is an inertial coordinate system comprised the vector ***E₁***, ***E₂*** and ***E₃***. The center of ***E*** is ***O*** that is fixed to the center of track. Starting from a reference to configuration, the normal to the track's plane is aligned ***E₃***. The track swing rotation by angle θ around ***E₂***,

$$\theta = \theta_0 \sin \pi \tau \tag{1}$$

where θ_0 is amplitude, τ is frequency of input vibration. We defined vector $\boldsymbol{e}_{t1}$, $\boldsymbol{e}_{t2}$ and $\boldsymbol{e}_{t3}$ from a right-handed orthogonal coordinate system $\boldsymbol{e}_t$ which corotates with the track. Vector $\boldsymbol{e}_{t2}$ is matched to $\mathbf{E}_2$, and the normal to the track's plane is aligned $\boldsymbol{e}_{t3}$.

The rotor precesses around $\boldsymbol{e}_{t3}$. We defined vectors $\boldsymbol{e}_1$, $\boldsymbol{e}_2$ and $\boldsymbol{e}_3$ from a right-handed orthogonal coordinate system $\boldsymbol{e}$ which corotates with precession of rotor. Vector $\boldsymbol{e}_3$ is matched to $\boldsymbol{e}_{t3}$, and $\boldsymbol{e}_2$ is located on the shaft. The top of the rotor axis contacts with an upper track in point P as shown in Figure 5. The $\boldsymbol{e}_\pi$ system is rotated $\boldsymbol{e}$ by –β that is angle between OP and $\boldsymbol{e}_1$ around $\boldsymbol{e}_2$. $\boldsymbol{e}_{\pi 2}$ is matched to $\boldsymbol{e}_2$, and $\boldsymbol{e}_{\pi 1}$ is matched to OP. We define ξ, that is

$$\xi = \frac{R_t}{R_a} = \frac{1}{\tan \beta} \tag{2}$$

where R_a is the radius of rotor, and R_t is the radius of track. If it is assumed that the shaft rolls the track without sliding, relationship between γ and α is

$$\dot{\gamma} = \xi \dot{\alpha} \tag{3}$$

where γ and α are spin and precession angles respectively. The angular velocity of the rotor $\boldsymbol{\omega}_r$ is calculated with the use of each coordinate system **E**, $\boldsymbol{e}_t$, $\boldsymbol{e}$, and $\boldsymbol{e}_\pi$.

$$\vec{\omega}_r = (\dot{\gamma} + \dot{\theta} \sin \alpha)\vec{e}_1 + (\dot{\theta} \cos \alpha)\vec{e}_2 + \dot{\alpha}\vec{e}_3 \tag{4}$$

The angular velocity $\boldsymbol{\Omega}$ of $\boldsymbol{e}$ system to $\boldsymbol{E}$ system is

$$\vec{\Omega} = (\dot{\theta} \sin \alpha)\vec{e}_1 + (\dot{\theta} \cos \alpha)\vec{e}_2 + \dot{\alpha}\vec{e}_3 \tag{5}$$

Because $\boldsymbol{e}$ system is corresponding to the inertia main axis of the rotor, rotor angular momentum $\boldsymbol{L}$ is

$$\vec{L} = I_1(\dot{\gamma} + \dot{\theta} \sin \alpha)\vec{e}_1 + I_2(\dot{\theta} \cos \alpha)\vec{e}_2 + I_2 \dot{\alpha}\vec{e}_3 \tag{6}$$

where I_1 is the principal moment of inertia about rotor's axis, and I_2 is the moment of inertia about orthogonal rotor's axis. The torque applied to the rotor is evinced,

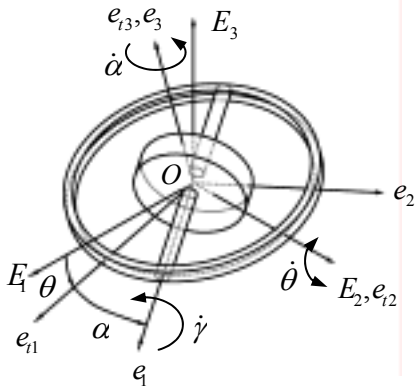

Fig.4 : Track and rotor coordinate

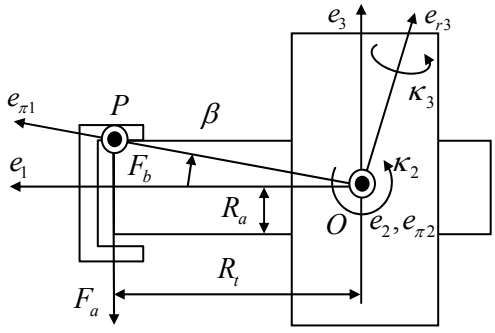

Fig.5 : Definition of e_π coordinate system.

$$\kappa_2 = 2F_a R_t \tag{7}$$

$$\kappa_3 = \frac{2F_b R_t}{\cos \beta} \tag{8}$$

where F_a is normal component of reaction, and F_b is frictional force as shown in Fig.5. The torque is represented as (9) using the moment against the rotation.

$$\vec{M} = \kappa_2 \vec{e}_{\pi 2} + \kappa_3 \vec{e}_{\pi 3} - \sigma \dot{\gamma} \vec{e}_1 \tag{9}$$

Substituting (3), (5), (6), and (9) into Euler's equation (10) obtained for ***e*** system, gives (11),(12),(13).

$$\vec{M} = \frac{\partial L}{\partial t} + \Omega \times L_1 \tag{10}$$

$$\ddot{\alpha}(\xi^2 I_1 + I_2) + \xi I_1 \ddot{\theta} \sin\alpha + (I_2 - I_1)\dot{\theta}^2 \sin\alpha\cos\alpha + \xi^2 \sigma\dot{\alpha} = 0 \tag{11}$$

$$I_2 \ddot{\theta}\cos\alpha + (I_1 - 2I_2)\dot{\theta}^2 \dot{\varepsilon}\sin\alpha + I_1 \xi\dot{\alpha}^2 = \kappa_2 \tag{12}$$

$$\ddot{\alpha}\xi(I_2 - I_1) - I_1\ddot{\theta}\sin\alpha - \dot{\alpha}\dot{\theta}(1+\xi)\cos\alpha + \xi(I_2 - I_1)\dot{\theta}\cos^2\alpha - \xi\sigma\dot{\alpha} = \frac{\kappa_3}{\sin\beta} \tag{13}$$

This is a nonlinear differential equation, and an analytical solution is not obtained. But the approximate solution in the steady state is obtained. In steady state the track vibration synchronizes with the rotor precession movement. If the rotation speed is assumed constant, the following condition stands

$$\alpha = \phi + \tau t \tag{14}$$

where ϕ is phase difference between α and θ. Substituting (14) and the relation that first and second differentials of ϕ are 0 into (11), and integrating it in a vibration cycle, the following equation is obtained.

$$\cos\phi = \frac{2\xi\sigma}{I_1\tau\theta_0} \tag{15}$$

Other unknowns, κ_2 and κ_3 are obtained from (12) and (13) which give the condition for non-slip rotation. This condition, however, stands automatically when the static friction coefficient is large enough. Thus we consider only Eqs. (11) or (15) from now on. The following condition is necessary so that Eq. (15) has a solution since $\cos\phi \leq 1$.

$$\sigma \leq \frac{I_1\theta_0\tau}{2\xi} \tag{16}$$

This expression gives the condition that the stationary rotation exists. Since generated electric power is proportional to electric damping coefficient σ, Eq. (16) decides the optimum value of σ.

4. TRANSIENT ANALYSIS

In this section, transient response of Eq. (11) is obtained numerically and the phase difference ϕ given by (14) is illustrated for various initial conditions. Figures 6 and 7 show time response of ϕ and $\dot{\phi}$ for the initial condition of $\phi = \dot{\phi} = 0$ where $\sigma = 6.0\times10^{-6}$ [kg・m^2/s], $I_1 = 6.3\times10^{-5}$ [kg・m^2], $\theta_0 = \frac{\pi}{3}$ [rad], $\tau = 4\pi$ [rad], $\xi = 40$.

These parameters satisfy stability condition (16). Fig. 6 and 7 show the results.

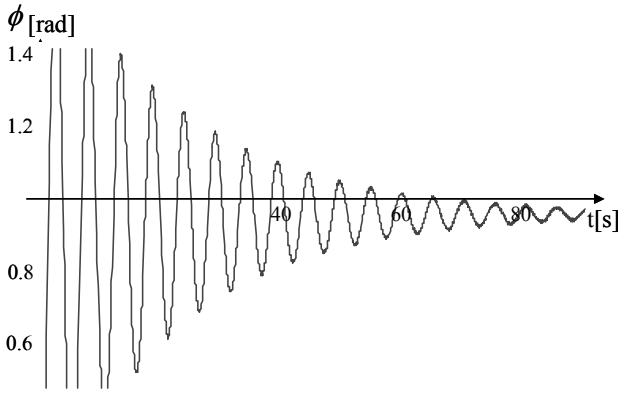

Fig.6 : Change of ϕ for stable rotation

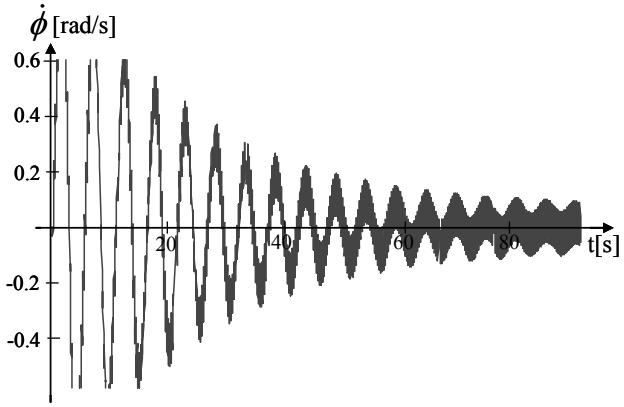

Fig.7 : Change of $\dot{\phi}$ for stable rotation

ϕ decreases with time and comes close to a certain value. $\dot{\phi}$ also decreases and becomes almost zero. These mean the rotor precession is synchronized with input vibration. But some fluctuations remain especially in $\dot{\phi}$ even after a long time. This happens because the input vibration is sinusoidal and gyroscopic torque changes in a precession cycle and precession speed changes by the torque change.

Figures 8 show results for the initial condition of ϕ=0 and $\dot{\phi}$=0.5π where other parameters are the same. In this case, ϕ decreases by the velocity -τ which means rotor stops rotation. This stall happens because initial condition is far from steady state condition.

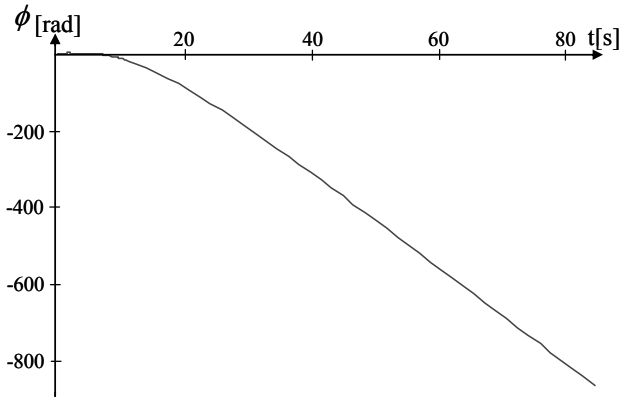

Fig.8 : Change of ϕ for unstable rotation

Figure 9 shows results for the initial conditions for ϕ=0 and $\dot{\phi}$=0.4π, 0.5π, 1.38π, 1.4π, 1.5π, 2.0π, 2.05π, 2.1π [rad/s] where ϕ and $\dot{\phi}$ are shown in a phase plane.

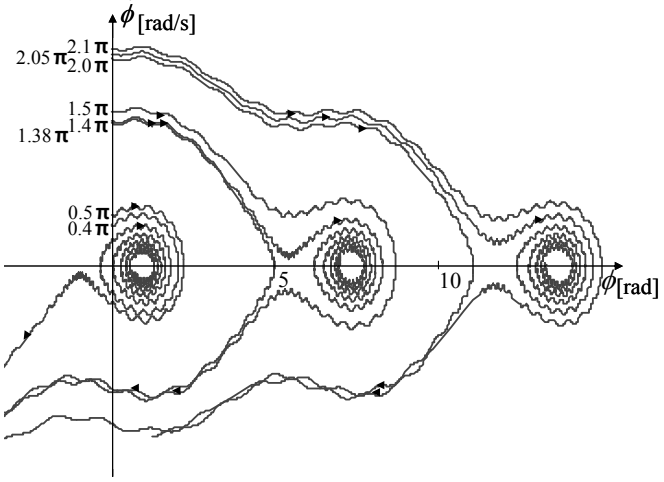

Fig.9 Phase curve of ϕ and $\dot{\phi}$ for large σ

Corresponding to the fluctuations of the graph in Fig. 7, there are small waves in lines whose frequency is 2Hz which is the same as τ. For initial conditions of $\dot{\phi}$=0.4π, 1.4π, 2.05π [rad/s], ϕ converges to around 0.95, 7.2, 13.5 which differs 2π each other and this means rotor rotates synchronized with input vibration at the same phase difference. For initial conditions of $\dot{\phi}$=0.5π, 1.38π, 1.5π, 2.0π, 2.1π [rad/s], phase curves go off to the minus infinity which means rotation stalls. These results show that initial conditions for stability exist discontinuously.
Approximate steady state solution (15) is shown by the mark ■. They are located at the center of the phase curves of stable conditions. This proves the correctness of our approximation method.

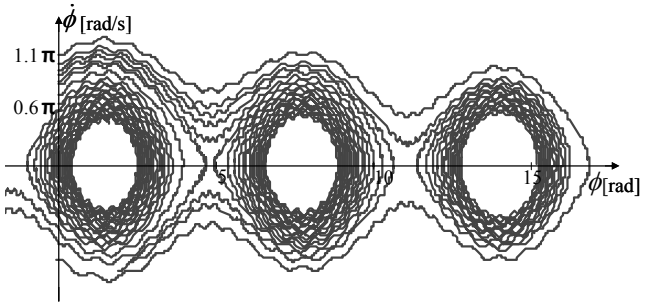

Fig.10: Phase curve of ϕ and $\dot{\phi}$ for small σ

Figure 10 shows results for $\sigma = 1.0 \times 10^{-6}$ which is lower than that of Fig. 10. Stable initial conditions are ϕ=0 and $0<\dot{\phi}<0.7\pi$ $0.81\pi<\dot{\phi}<0.86\pi$ $0.98\pi<\dot{\phi}<\pi$ which means stability of the system is increased. This qualitatively corresponds to Eq. (16) which shows there exists upper limit of σ for stable rotation.

4. CONCLUSION

To clarify the stability conditions of the gyroscopic power generator, steady state and transient analyses of rotor precession are analyzed. Main results are shown below.

- When suitable initial angles and angular velocities are given to the rotor, rotation converges to stable condition. The stable initial conditions exist discontinuously.
- Even in a steady state, a small vibration of input frequency remains in the rotor precession. Approximate solution for the steady state exists at the center of remaining vibration area in the phase plane.
- According to the approximate solution for the steady state, there exists upper limit of electrical damping for stable rotation. This was verified by numerical analyses.

REFERENCES

[1] Shad Roundy, Paul Kenneth, Jan M. Rabaey : Energy Scavenging for Wireless Sensor Networks with Special Focus on Vibrations, Kluwer Academic Publishers, Nowell, 2004.
[2] Tomohiro Ishii, Yuji Goto, Tatsuya Ogawa, and Hiroshi Hosaka : Development of a gyroscopic power generator using human vibration, Journal of the Japan Society of Precision Engineering, **74**, 7 (2008), pp.764-768, in Japanese
[3] Archie L. Mishler, Gyroscopic Device, United States Patent 3726146, Apr. 10, 1973
[4] D.W. Gulick, O.M.O'Reilly : On the Dynamics of the Dynabee, J. of Applied Mechanics, **67**, (2000), pp. 321-325